

RESEARCH

Open Access



Treatment of adult ALL patients with third-generation CD19-directed CAR T cells: results of a pivotal trial

Maria-Luisa Schubert¹, Anita Schmitt¹, Angela Hückelhoven-Krauss¹, Brigitte Neuber¹, Alexander Kunz¹, Philip Waldhoff¹, Dominik Vonficht^{2,3,4}, Schayan Yousefian^{5,6,7}, Lea Jopp-Saile^{2,3,4}, Lei Wang¹, Felix Korell¹, Anna Keib¹, Birgit Michels¹, Dominik Haas¹, Tim Sauer¹, Patrick Derigs¹, Andreas Kulozik⁸, Joachim Kunz⁸, Petra Pavel⁹, Sascha Laier⁹, Patrick Wuchter¹⁰, Johann Schmier¹¹, Gesine Bug¹², Fabian Lang¹², Nicola Gökbüget¹², Jochen Casper¹³, Martin Görner¹⁴, Jürgen Finke¹⁵, Andreas Neubauer¹⁶, Mark Ringhoffer¹⁷, Denise Wolleschak¹⁸, Monika Brüggemann¹⁹, Simon Haas^{2,3,5,6,7,20}, Anthony D. Ho^{1,20}, Carsten Müller-Tidow^{1,20}, Peter Dreger^{1,20} and Michael Schmitt^{1,20*}

Abstract

Background Third-generation chimeric antigen receptor (CAR)-engineered T cells (CARTs) might improve clinical outcome of patients with B cell malignancies. This is the first report on a third-generation CART dose-escalating, phase-1/2 investigator-initiated trial treating adult patients with refractory and/or relapsed (r/r) acute lymphoblastic leukemia (ALL).

Methods Thirteen patients were treated with escalating doses of CD19-directed CARTs between 1×10^6 and 50×10^6 CARTs/m². Leukapheresis, manufacturing and administration of CARTs were performed in-house.

Results For all patients, CART manufacturing was feasible. None of the patients developed any grade of Immune effector cell-associated neurotoxicity syndrome (ICANS) or a higher-grade (\geq grade III) cytokine release syndrome (CRS). CART expansion and long-term CART persistence were evident in the peripheral blood (PB) of evaluable patients. At end of study on day 90 after CARTs, ten patients were evaluable for response: Eight patients (80%) achieved a complete remission (CR), including five patients (50%) with minimal residual disease (MRD)-negative CR. Response and outcome were associated with the administered CART dose. At 1-year follow-up, median overall survival was not reached and progression-free survival (PFS) was 38%. Median PFS was reached on day 120. Lack of CD39-expression on memory-like T cells was more frequent in CART products of responders when compared to CART products of non-responders. After CART administration, higher CD8+ and $\gamma\delta$ -T cell frequencies, a physiological pattern of immune cells and lower monocyte counts in the PB were associated with response.

Conclusion In conclusion, third-generation CARTs were associated with promising clinical efficacy and remarkably low procedure-specific toxicity, thereby opening new therapeutic perspectives for patients with r/r ALL.

Trial registration This trial was registered at www.clinicaltrials.gov as NCT03676504.

*Correspondence:

Michael Schmitt

michael.schmitt@med.uni-heidelberg.de

Full list of author information is available at the end of the article



© The Author(s) 2023. **Open Access** This article is licensed under a Creative Commons Attribution 4.0 International License, which permits use, sharing, adaptation, distribution and reproduction in any medium or format, as long as you give appropriate credit to the original author(s) and the source, provide a link to the Creative Commons licence, and indicate if changes were made. The images or other third party material in this article are included in the article's Creative Commons licence, unless indicated otherwise in a credit line to the material. If material is not included in the article's Creative Commons licence and your intended use is not permitted by statutory regulation or exceeds the permitted use, you will need to obtain permission directly from the copyright holder. To view a copy of this licence, visit <http://creativecommons.org/licenses/by/4.0/>. The Creative Commons Public Domain Dedication waiver (<http://creativecommons.org/publicdomain/zero/1.0/>) applies to the data made available in this article, unless otherwise stated in a credit line to the data.

Keywords Acute lymphoblastic leukemia (ALL), Third-generation chimeric antigen receptor (CAR) T cells, Investigator-initiated trial (IIT), CART-associated toxicities, Cytokine release syndrome (CRS), Cytopenia, Immune effector cell-associated neurotoxicity syndrome (ICANS), CD39

Introduction

Chimeric antigen receptor T cell (CAR) products targeting CD19 have been approved for the treatment of patients with relapsed and/or refractory (r/r) B cell malignancies [1–4], including patients with acute lymphoblastic leukemia (ALL) [2, 3].

All commercially available CARTs express second-generation CARs that contain one costimulatory domain. Third-generation CARTs comprising two costimulatory domains have shown superior engraftment, improved expansion capacity and prolonged persistence [5–9]. Clinically, superior expansion and longer persistence were observed when CD19-directed second (CD28 costimulatory domain)- and third-generation (CD28 and 4-1BB) CARTs were simultaneously administered to lymphoma patients [10]. However, clinical data evaluating solely third-generation CARTs are limited [11].

Here, we describe the first results obtained with an academically developed third-generation CAR in the framework of the investigator-initiated trial (IIT) Heidelberg CAR number 1 (HD-CAR-1) in adult patients with r/r ALL. All steps of treatment including leukapheresis, manufacturing and administration of CARTs, patient monitoring as well as patient follow-up were performed in-house.

A solely academic-driven trial, a third-generation Good Manufacturing Practice (GMP) grade retroviral vector and treatment of adult r/r ALL patients with escalating CART doses make this trial hitherto unique.

Methods

Study design

Adult patients with confirmed CD19-positive, minimal residual disease (MRD)-positive, hematological or extramedullary r/r ALL received escalating doses of autologous T-lymphocytes retrovirally transduced with a third-generation CD19-directed CAR (RV-SFG.CD19.CD28.4-1BBzeta) [12]. Endpoints included feasibility of manufacturing and treatment safety, clinical efficacy and survival. Patients were evaluated as outlined in the study calendar [12]. Written informed consent was obtained from all patients prior to treatment. The trial was conducted according to the principles of the Declaration of Helsinki.

HD-CAR-1 CART manufacturing

As described [12, 13], patients underwent leukapheresis for collection of peripheral blood mononuclear cells (PBMCs). PBMCs were transduced with RV-SFG.CD19.CD28.4-1BBzeta retroviral vector supernatant supernatant (provided by Prof. Malcolm Brenner, Baylor College of Medicine, Houston, Texas, USA) after three days of activation with anti-CD3 and anti-CD28 antibodies (MACS GMP Pure, Miltenyi Biotec, Bergisch Gladbach, Germany). RV-SFG.CD19.CD28.4-1BBzeta carries an anti-CD19 scFv derived from the FMC63 antibody inserted to the SFG retroviral backbone. The transmembrane domain is derived from CD28, the hinge domain from the human IgG1-CH2CH3 domain and 4-1BB is inserted between the CD28 and CD3 ζ (CAR structure displayed in Additional file 1: Figure S1). Transduced cells were cultured in complete medium supplied with interleukine (IL)-7 (10 ng/mL) and IL-15 (5 ng/mL) (CellGenix, Freiburg, Germany) for a total of 13 days at the GMP Core Facility of the Internal Medicine V Department of the Heidelberg University Hospital (were evaluated) as described [12]. Medium change was performed on days 7 and 10. Cells were cryopreserved using an automated device (Biofreeze BV 40 Consarctic, Westerngrund, Germany). Transduction efficiency was assessed using flow cytometry (FACS Canto, BD Biosciences, Franklin Lakes, NJ, USA). After testing for sterility (Ph. Eur. 2.6.1), mycoplasma (Ph. Eur. 2.6.7) and endotoxin (Ph. Eur. 2.6.14), products were released for administration.

CART treatment and follow-up, evaluation of toxicity and outcome

Patients received the respective dose of HD-CAR-1 CARTs on day 0 after lymphodepletion (fludarabine 90 mg/m² and cyclophosphamide 1500 mg/m²). Cytokine release syndrome (CRS) and immune effector cell-associated neurotoxicity syndrome (ICANS) were graded according to the consensus guidelines of the American Society for Transplantation and Cellular Therapy (ASTCT) [14] and managed according to institutional guidelines and as published [15]. Tumor lysis syndrome (TLS) was graded as described [16]. Adverse events (AEs) were graded according to the National Cancer Institute Common Terminology Criteria for

Adverse Events (CTCAE), version 5.0. B cell aplasia was defined as B cell count in the PB below 100/ μ l as assessed by flow cytometry. Lymphodepletion, CART administration and safety monitoring were performed as inpatient procedures with mandatory hospitalization from day -6 through day +14. Following patient discharge, patients presented in the outpatient department according to the study visit schedule [12].

Clinical efficacy of HD-CAR-1 treatment was assessed according to response criteria defined for ALL [17, 18], i.e., bone marrow (BM) aspiration and/or radiologic imaging in case of extramedullary disease.

Assessment of CART frequencies

HD-CAR-1 CART frequencies were quantified by single-copy gene (SCG)-based duplex quantitative PCR (SCG-DP-PCR) amplifying simultaneously the human SCG ribonuclease (RNase) P RNA component H1 (RPPH1) and the FMC63 domain of the CAR transgene as described [19].

Assessment of cellular composition of CART products and patient samples

Flow cytometry

From ten HD-CAR-1 patients (unique patient number (UPN)#1-#7 and UPN#9-#11), PBMCs of the manufactured CART product and of peripheral blood (PB) samples collected after CART treatment were analyzed using 35-parametric spectral flow cytometry analysis. PBMCs derived from buffy coats of three healthy donors served as controls (used antibodies summarized in Additional file 1: Table S1).

Computational analysis

Spectral unmixing of obtained data was performed using SpectroFlow (Cytek Biosciences). For general downstream analysis, the R packages Spectre [20], CATALYST [21] and diffcyt [22] were used.

Using the Spectre package, CART product and PBMC data were merged into a single data table, with keywords denoting the sample, group and other metadata added to each row (cell). Since data were acquired over the course of two days, batch alignment was performed by computing quantile conversions using reference samples recorded with each batch, and then applied to the samples in each batch using CytoNorm [23] in Spectre. The batch-corrected values were used for all downstream computations including clustering and differential expression analyses.

Analysis of T cells: For detailed clustering and subset annotation of individual T cell populations (CD4+ and

CD8+T cells), the cluster function from the CATALYST package [21] (version 1.18.1) was used, which performs a FlowSOM clustering and ConsensusClusterPlus metaclustering. Markers that were included for clustering were specified and were dependent on the respective T cell population excluding cells expressing the CAR.

For cellular visualizations, the dimensionality reduction algorithm Uniform manifold approximation and projection (UMAP) [24] was used on downsampled data, taking surface expression of used markers into consideration.

Analysis of CAR T cells: For analysis of CD4+ or CD8+ CARTs, the CD4+ and CD8+ T cell clusters were selected and the surface expression of the CAR detection marker was used to gate CAR+ T cells. Within the CD4+ or CD8+ T cell compartments, cells were gated using the same cutoffs for every sample. Due to spectral spillover, different cutoffs for the CD4+ and CD8+ compartment were applied.

For principal component analysis (PCA), the cell-type frequencies for each sample were used as input. Cell-type frequencies were calculated sample-wise by dividing the number of cells of per population by the total number of cells within that sample.

To perform differential expression analysis, the diffcyt package [22] (version 1.14.0) was used. The models and contrast matrices were set up with the createFormula and createContrast functions from the diffcyt package. For the differential abundance analysis, a generalized linear mixed model (GLMM) was used and adjusted *p* values (based on Benjamini–Hochberg [25] method) were returned. For differential expression analysis of CD39 on cells of non-responders or responders, a linear mixed model (LMM) was applied and the unadjusted *p* value was reported.

Differential abundance analyses were performed by calculating the frequency of cells per population out of the total CD45+ cells per sample or the frequency of cells per CD4+ or CD8+ T cell subset out of all CD3+TCRab+ T cells, respectively. For comparisons of responders versus non-responders, the mean frequency for every population in non-responders was calculated. Then, frequencies for every population in responders were divided by the corresponding mean frequency from non-responders as determined in the step before. Likewise, for comparisons of CART recipients versus healthy donors, the mean frequency for every population in healthy donors was calculated. Then, frequencies for every population in CAR recipients were divided by the corresponding mean frequency from non-responders as determined in the step before. Sample-specific fold changes were \log_2 -transformed and visualized as boxplots.

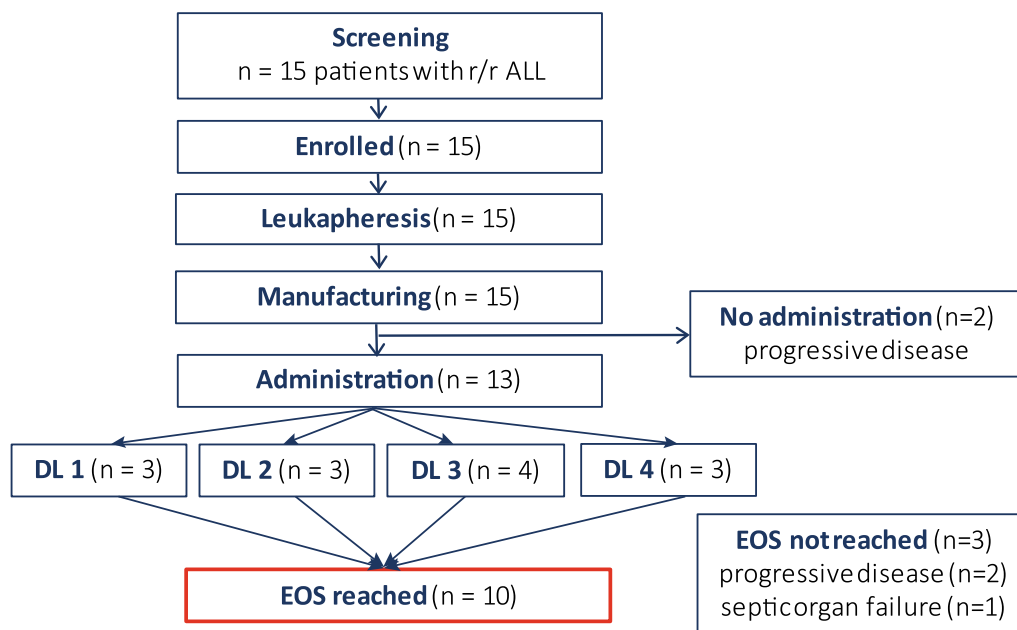


Fig. 1 HD-CAR-1 study profile. Fifteen patients with relapsed and/or refractory (r/r) acute lymphoblastic leukemia (ALL) after at least two prior therapy lines were screened and enrolled into HD-CAR-1. For all patients, leukapheresis and manufacturing of CARTs were feasible. Two patients did not receive the HD-CAR-1 CART product due to progressive disease (PD). Thirteen patients were treated with CARTs, with three patients receiving 1×10^6 (dose level (DL) 1), three patients 5×10^6 (DL2), four patients 20×10^6 (DL3) and three patients 5×10^7 (DL4) CARTs/m². Ten patients reached end of study (EOS) on day 90 after CART administration. Three patients died due to progressive disease ($n=2$) or due to septic organ failure ($n=1$) prior to EOS

Statistical analysis

Statistics were calculated using Prism Software (GraphPad Software Inc., version 8.2.2). Progression-free survival (PFS) was calculated from the date of CART administration until the date of clinical progression, relapse or death, respectively. Differences between survival curves were descriptively calculated by log-rank testing. A p value <0.05 was considered statistically significant.

Results

Patient characteristics

Between September 2018 and January 2022, 15 patients with r/r ALL were enrolled (Fig. 1). The patient baseline characteristics are detailed in Table 1. Median age of patients was 41 (range 21–67) years. Median time from initial diagnosis to CART administration was 22 (range 5–117) months, and patients had received a median of 4 (range 2–9) prior treatment lines, including allogeneic stem cell transplantation (alloSCT) in 12 patients (80%). None of the patients received immune suppression at the time of leukapheresis or had signs of active graft-versus host disease (GvHD). All patients were complete donor chimeras at the time of leukapheresis.

Feasibility of HD-CAR-1 CART manufacturing

Leukapheresis and manufacturing of CARTs were successful for all enrolled patients. Due to low T cell counts in the PB of one patient (UPN#12), two consecutive CART production cycles had to be performed. Median duration of CART manufacturing was 10 (range 10–14) days. Median transduction efficiency was 52.7% (range 39.3–66.9%) with a viability of CARTs of $>85\%$. CART production details are summarized in Additional file 1: Table S2.

CART administration

Of 15 patients, six patients received bridging therapy between leukapheresis and lymphodepleting therapy. Thirteen patients received HD-CAR-1 CARTs. (UPN#14 and UPN#15 did not receive CARTs due to progressive disease (PD) during CART manufacturing.) Three patients were treated with CARTs at dose level (DL) 1 (1×10^6 CARTs/m²), DL2 (5×10^6 CARTs/m²) and DL4 (5×10^7 CARTs/m²). Four patients were treated at DL3 (2×10^7 CARTs/m²) (Fig. 1). Ten patients reached end of study (EOS) on day 90 after CARTs. Three patients did not reach EOS due to PD ($n=2$) at day 23 (UPN#8) and day 76 (UPN#3), respectively, and due to fatal septic organ failure ($n=1$; UPN#12) on day 39 (Table 2).

Table 1 Patient characteristics

UPN	Age	Gender	Disease	Extra-medullary disease prior CARTs	Diagnosis to CARTs [months]	# Prior tx lines	Prior alloSCT/donor/source	Prior blina	Bridging*	Disease status at LD
1	32	F	B-ALL	Yes (CNS)	117	9	Yes (2x)/2x MUD/2 x PBSCT	Yes	Yes	CSF: 7 blasts / μ l; BM: <5% blasts, MRD -
2	21	M	Pre-B-ALL	No	15	4	Yes/MUD/PBSCT	Yes	No	Molecular relapse (BM MRD 0.3%)
3	67	F	B-ALL	No	15	2	No	No	No	Molecular relapse (BM MRD 0.3%)
4	32	F	B-ALL	No	8	2	Yes/MUD/PBSCT	No	No	6% blasts in BM
5	63	M	Pre-B-ALL	No	20	4	Yes/haplo/BMT	Yes	No	8% blasts in BM
6	28	F	B-ALL	Yes (bone)	22	7	Yes/MUD/PBSCT	No	No	PD (right epicondyle, humerus)
7	67	F	MPAL	No	97	4	Yes/MUD/PBSCT	No	Yes	Molecular relapse (BM MRD 0.018%)
8	36	F	Pre-B-ALL	Yes (left mamma, parotid gland, lymph nodes (axillary, mediastinal, parailiacal, inguinal)	8	5	No	Yes	Yes	48% blasts in BM and PD of extramedullary disease
9	45	M	B-ALL	No	25	6	Yes/MUD/PBSCT	No	No	Molecular relapse (BM MRD 0.36%)
10	47	F	B-ALL	No	18	4	Yes/MUD/PBSCT	Yes	No	Molecular relapse (BM MRD 0.3%)
11	37	M	B-ALL	No	52	5	Yes/MUD/PBSCT	Yes	No	BM blasts 6%
12	36	M	B-ALL	Yes (kidney, liver, bone)	28	4	Yes/MMUD/PBSCT	Yes	No	PR of extramedullary manifestations, BM: <5% blasts
13	32	M	B-ALL	Yes (bone)	117	4	Yes/MUD/PBSCT	Yes	Yes	PD of extramedullary manifestations (10 th rib, both femurs, both tibiae, left Os ilium), BM: <5% blasts
14 [§]	47	M	B-ALL	No	41	4	Yes/MMUD/PBSCT	Yes	Yes	Molecular relapse (BM MRD 0.3%)/death due to PD prior LD
15 [§]	65	M	B-ALL	No	5	3	No	Yes	Yes	8% blasts in BM/death due to sepsis prior LD

ALL acute lymphoblastic leukemia, alloSCT allogeneic stem cell transplantation, B-ALL common B cell leukemia, BM bone marrow, BMT bone marrow transplant, CART chimeric antigen receptor T cells, CNS central nervous system, CR complete remission, CSF cerebrospinal fluid, F female, haplo haploidentical hematopoietic stem cell transplantation, LD lymphodepletion, M male, MPAL mixed-phenotype acute leukemia, MRD minimal residual disease, MMUD HLA-mismatched unrelated donor, MUD HLA-matched unrelated donor, PBSCT peripheral blood stem cell transplant, PR partial remission, pre-B-ALL precursor B cell acute lymphoblastic leukemia, PD progressive disease, SD stable disease, tx therapy, UPN unique patient number

*Treatment administered between leukapheresis and lymphodepletion

[§] Patients #14 and #15 did not receive HD-CAR-1 CARTs

Table 2 Toxicity and clinical response to treatment with the HD-CAR-1 product

UPN	Age	Gender	Disease	CART dose [CARTs/m ²]	CRS grade	ICANS	Infection	Best response	Response at EOS	alloSCT after CARTs	Progression of disease/death [day after CARTs]
1	32	F	B-ALL	1 × 10 ⁶	I	-	RSV	PD	PD	-	28 (CSF: 13 blasts /μl)/254
2	21	M	Pre-B-ALL	1 × 10 ⁶	-	-	-	CR MRD+	CR MRD+	Yes	119 (BM: 8% blasts)/268
3 [†]	67	F	B-ALL	1 × 10 ⁶	-	-	-	CR MRD+ (day 28)	n.r.	-	56 (BM: 52% blasts)/76
4	32	F	B-ALL	5 × 10 ⁶	-	-	-	CR MRD-	CR MRD-	-	-
5	63	M	Pre-B-ALL	5 × 10 ⁶	-	-	<i>Staph. epi</i>	CR MRD-	CR MRD+	-	146 (extramedullary: malignant ascites)
6	28	F	B-ALL	5 × 10 ⁶	I	-	-	CR MRD-	CR MRD-(metabolic CR)	-	120 (extramedullary: right mamma)
7	67	F	MPAL	20 × 10 ⁶	-	-	-	CR MRD-	CR MRD+	-	-
8 [†]	36	F	Pre-B-ALL	20 × 10 ⁶	II	-	-	PD	n.r.	Yes	23 (BM: 100% blast infiltration)/58
9	45	M	B-ALL	20 × 10 ⁶	-	-	-	CR MRD-	CR MRD-	-	189 (CSF: 50–60% blasts)
10	47	F	B-ALL	20 × 10 ⁶	-	-	-	CR MRD+	PD	Yes	93 (BM: 9% blasts)
11	37	M	B-ALL	50 × 10 ⁶	-	-	Respiratory*	CR MRD-	CR MRD-	-	-
12 [†]	36	M	B-ALL	50 × 10 ⁶	II	-	<i>E. coli</i> sepsis	SD (day 26)	n.r.	-	-/39 (TRM: septic MOV)
13	32	M	B-ALL	50 × 10 ⁶	-	-	Respiratory*	CR MRD-	CR MRD-(metabolic CR)	-	-

ALL acute lymphoblastic leukemia, BM bone marrow, c-ALL common B cell leukemia, CART chimeric antigen receptor T cells, CR complete remission, CRS cytokine release syndrome, CSF cerebrospinal fluid, EOS end of study on day 90 after HD-CAR-1 treatment, F female, M male, MPAL mixed-phenotype acute leukemia, MOV multi-organ failure, MRD minimal residual disease, n.r. not reached, pre-ALL precursor B cell acute lymphoblastic leukemia, PD progressive disease, RSV respiratory syncytial virus, SD stable disease, TRM treatment-related mortality, UPN unique patient number

[†] Patient died before reaching EOS

*No pathogen identified

Safety

CRS/ICANS

Treatment with HD-CAR-1 CARTs was well tolerated (Table 2): None of the patients developed ICANS. Two patients (UPN#1 and UPN#6) developed grade I CRS with symptoms limited to fever that resolved with supportive treatment only and two patients (UPN#8, UPN#12) developed grade II CRS and received treatment with tocilizumab. UPN #8 additionally received steroids. One patient (UPN#5) developed febrile temperatures eventually attributable to *Staph. epidermidis* bacteremia that resolved with targeted antibiotic treatment (Additional file 1: Table S3). Higher-grade CRS, i.e., grade \geq III, was not observed in any patient.

Patient #8, who suffered from multiple extramedullary ALL lesions prior treatment (Table 1), developed fever and mild hypoxia three days after CART administration suggestive for CRS. With high ferritin, triglycerides and sCD25, a concomitant hemophagocytic lymphohistiocytosis (HLH)/macrophage activation syndrome (MAS) was suspected. Several doses of tocilizumab and steroids were administered. Due to further clinical deterioration including kidney failure, eventually PD was suspected. A BM biopsy performed on day 10 confirmed PD with almost 100% infiltration of the BM with ALL blasts. CRS symptoms and kidney failure were retrospectively attributed to an overlapping TLS. The patient was subsequently treated with inotuzumab-ozogamicin and received an alloSCT from a matched-related donor, but eventually died 58 days after CART infusion.

Patient #12 received CARTs 16 months after a mismatched unrelated donor alloSCT that had been complicated by a grade 3 gastrointestinal (GI) GvHD [26]. On day 8, the patient developed CRS grade II and received tocilizumab. On day 19, the patient displayed an enterocolitis that evolved into an *E. coli* sepsis and progressed to septic shock with disseminated intravascular coagulation (DIC) and multi-organ failure. The patient died on day 39. Autopsy revealed that the enterocolitis had most probably been provoked and aggravated by GI-GvHD exacerbation. Elevated CART expansion was neither observed in the afflicted parts of the gut mucosa, nor in ascites/pleural effusion as proven by post-mortem quantitative PCR.

Cytopenia, B cell aplasia and infectious complications

Cytopenia, B cell aplasia and recovery of neutrophil counts are depicted in Fig. 2A, B. Persistent, i.e., beyond EOS, high-grade (\geq III) neutropenia was observed in two of nine evaluable patients (22%). Grade III neutropenia and thrombocytopenia were observed in UPN#4 who had low blood counts already before CARTs. Grade III

neutropenia in UPN#2 persisted until an alloSCT, which was performed on day 126. No higher-grade anemia was observed.

Ten patients (77%) had low B cell counts already prior CARTs, most likely due to pretreatment with blinatumomab ($n=8$) or cytoreductive bridging treatment ($n=4$) (Table 1). At EOS, all evaluable patients ($n=9$; UPN#9 not shown due to PD at EOS) had ongoing B cell aplasia (Fig. 2A), even though recovered levels of immunoglobulins were detectable in six patients (data not shown).

Until EOS, two patients (UPN#11 and UPN#13) developed respiratory infections that required oral antibiotics. One patient (UPN#1) was diagnosed with respiratory syncytial virus (RSV) that resolved with supportive care only. No patient with a prior alloSCT reactivated with cytomegalovirus (CMV) or Epstein–Barr virus (EBV).

Other toxicities

Two patients who had undergone a prior alloSCT developed GvHD after CART treatment. UPN#6 displayed a GvHD of the lung, and a preexisting GvHD of the GI tract exacerbated in UPN#12 (see above). No non-hematologic (\geq grade III toxicity not preexisting or attributed to underlying malignancy) or hematologic (grade IV cytopenia (except lymphopenia) persisting beyond day 30 post-CARTs) dose-limiting toxicity (DLT) occurred. Toxicities after CAR T cells showed no association with the administered CAR T cell dose. Toxicities are summarized in Additional file 1: Table S3.

Outcomes

Overall, ten patients (77%) achieved a complete remission (CR) as best response. Seven patients (54%) attained MRD negativity. At EOS, 10 patients were evaluable for response: eight patients (80%) achieved CR, with five patients (50%) confirmed to be MRD-negative. Median overall survival (OS) at 12-month follow-up was not reached (Fig. 3A), and median PFS was reached on day 120 (Fig. 3B). In patients who achieved a MRD-negative CR at EOS ($n=5$), 100% OS (Fig. 3C) and 60% PFS (Fig. 3D) at 1-year follow-up were higher compared to patients that failed MRD clearance ($n=8$) (OS 38%; PFS 12.5%; OS $p=0.08$; PFS $p=0.0047$). Three patients received a second CART administration (UPN#1, #4, #6) that eventually mediated MRD-negative CR in two patients (UPN#4 and UPN#6). Three patients underwent alloSCT after HD-CAR-1 treatment (first alloSCT, $n=1$ (UPN#8); second alloSCT, $n=2$ (UPN#2, UPN#10)). Evolution of patients within one year after HD-CAR-1 treatment is depicted in Fig. 3E. Of the patients that reached EOS ($n=10$), two patients have died from PD (UPN#1)

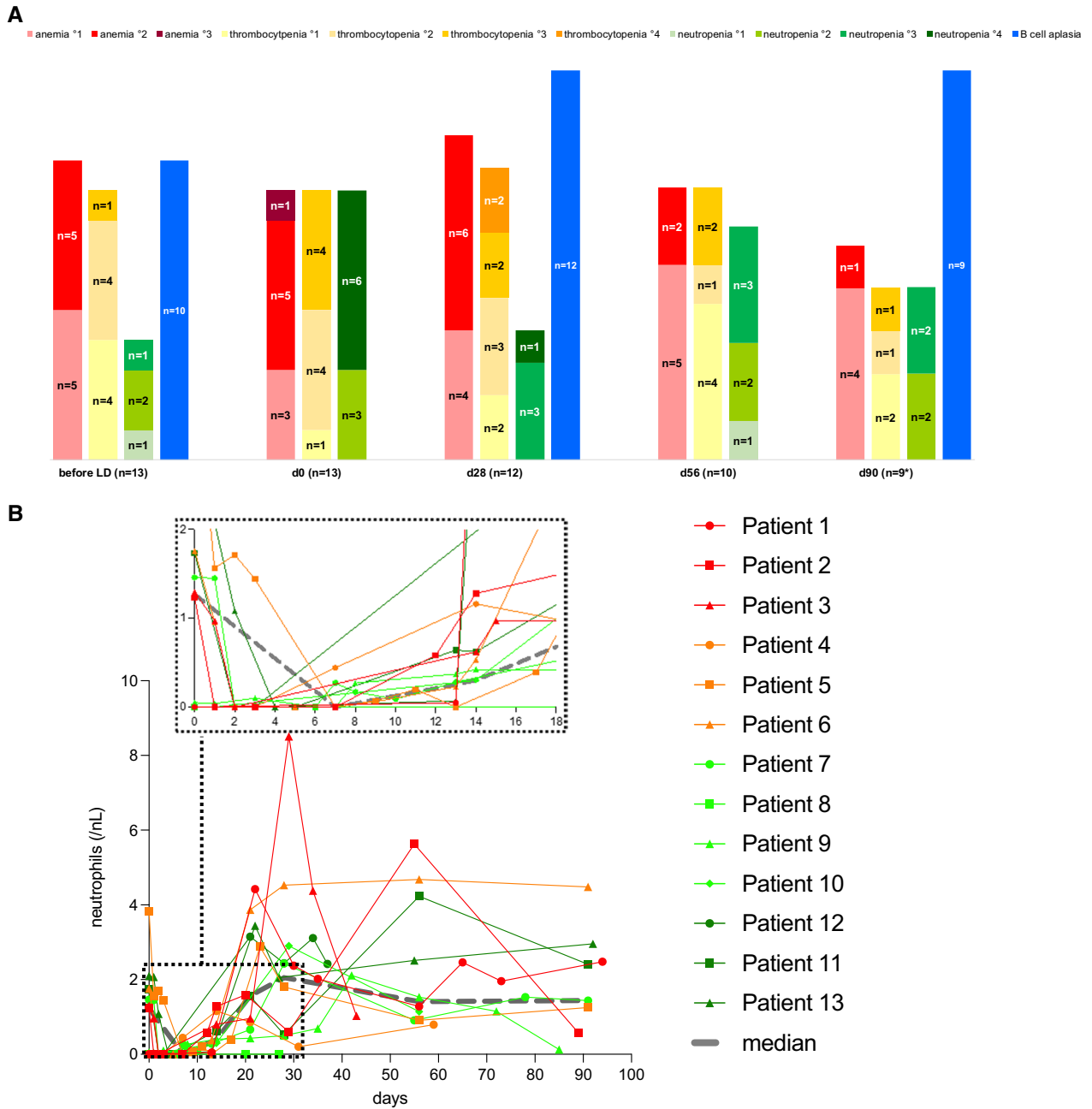


Fig. 2 Hematologic toxicity of HD-CAR-1 treatment. **A** Cytopenia and B cell aplasia. On day 0, i.e., after lymphodepletion (LD) and before CART administration, 69% ($n=9$) of patients were neutropenic (46% grade IV neutropenia), anemic (8% grade III anemia) and thrombocytopenic (31% grade III thrombocytopenia). One month after HD-CAR-1 treatment, 8% ($n=1$, UPN#4) patients displayed grade IV neutropenia and 17% ($n=2$; UPN#4 and UPN#11) grade IV thrombocytopenia. On end-of-study (EOS) at day 90, two patients showed persistent grade III neutropenia (UPN#2, UPN #4) and one patient grade III thrombocytopenia (UPN#4) despite treatment with granulocyte-colony-stimulating factor (G-CSF) and a thrombopoietin-agonist, respectively. (UPN#4 had grade III neutropenia and thrombocytopenia already before receiving CARTs; also, UPN#2 was already neutropenic before CART treatment.) No higher-grade anemia was observed. Beyond day 28, no grade IV cytopenia was observed. As for B cell counts, 77% ($n=10$) of patients displayed B cell aplasia already before receiving CARTs. At EOS, all evaluable patients ($n=9$; UPN#9 not shown due to PD) had ongoing B cell aplasia (B cell count on day 0 and day 56 not assessed). **B** Absolute neutrophil count (ANC) of treated HD-CAR-1 patients ($n=13$) within the first 18 days (top, small frame) and up to end of study on day 90 after CART treatment. Four patients (UPN #1, #3, #4, #11, #13) received G-CSF after CARTs. Median of ANCs is depicted in grey

and complications after an alloSCT (UPN#2), respectively, two patients are alive with disease (UPN #5,10), two patients are in MRD-positive (UPN#7,9) and four patients in MRD-negative CR (UPN#4,6,11,13). With exception of UPN#6, relapses remained positive for CD19 expression (UPN#3 not assessed for CD19 status at relapse).

Response to treatment was associated with CART doses: Patients that were treated with higher CART doses, i.e., DL3 and DL4, showed a trend toward superior OS (Fig. 3F) and PFS (Fig. 3G) compared to patients that received lower CART doses, i.e., DL1 and DL2.

CART expansion

PB CART expansion was observed in all patients immediately after CART administration. At EOS, CARTs were still detectable in seven (78%) of the evaluable patients (Fig. 4A). Higher CART doses (DL3, DL4) resulted in higher and prolonged expansion levels, whereas loss of detection occurred in patients that had received lower CART doses (DL1: UPN#1, #3, DL2: UPN#6) (Fig. 4B). Patients reaching expansion levels exceeding the median of 22.350 CART/ μ g DNA PBMC within the first month after treatment were more likely to respond than patients who displayed CART expansion below the median (Fig. 4C).

Cellular landscape of the CART product and the PB of patients after CART treatment

We used high-dimensional flow cytometry to characterize CART products (Fig. 5) and PB composition (Fig. 6) of treated patients. The CART product of analyzed patients ($n=10$) contained mostly CD4+ and CD8+ T cells. Also, minor fractions of $\gamma\delta$ -T cells and natural killer (NK) cells were identified (Fig. 5A, Additional file 1: Fig. S1A). All CART products contained CAR-positive T cells (Additional file 1: Table S2). Unsupervised clustering and dimensionality reduction of the CD4+ and CD8+ T cell compartments revealed differences in the cellular composition of the CART product in responders and non-responders (Fig. 5B, C): In responders, higher frequencies of CD39-negative effector memory-like CD4+ and CD8+ T cells were observed, whereas

non-responders displayed higher levels of CD39-positive effector memory-like T cells (Fig. 5C, D, F). In fact, CD39 expression of all T cells in both CD4+ and CD8+ CART product subsets was elevated in non-responders (Fig. 5E, G), suggesting association of CD39 expression in the CART product with positive therapeutic outcome.

As for analysis of PBMCs obtained after CART administration, non-responders displayed elevated levels of monocytes, whereas responders showed a tendency toward higher CD8+ T cell and $\gamma\delta$ -T cell frequencies (Fig. 6A, B). Expectedly, B cells in the highly-pretreated CART recipients were almost completely absent when compared to healthy donors (Additional file 1: S2B and Fig. 2A). Notably, the cellular landscape of patient #11 who remains in ongoing CR after CARTs (without further treatment (Fig. 3E)) was similar to the physiological cellular composition of healthy donors (Additional file 1: S2F). Unsupervised clustering and dimensionality reduction of CD4+ and CD8+ T cell subsets revealed well-known T cell differentiation states of CAR-negative, endogenous T cells and CAR-positive T cells (Fig. 6C, D). Both CD4+ and CD8+ CARTs of responders adopted to a higher degree effector memory and effector T cell states, whereas CARTs of non-responders predominantly adopted central memory phenotypes with high PD-1 expression (Fig. 6E, F). Similar findings were observed in the endogenous T cell compartments (Additional file 1: Fig. S2C–E).

Discussion

Despite novel therapeutic options for treatment of r/r ALL patients [27–29], the outcome for older patients remains poor [30–32]. Here, we treated adult ALL patients with escalating doses of CD19-specific third-generation CARTs. For all patients, CART products were successfully manufactured. Despite low CART doses administered and a heavily pre-treated patient cohort, a CR rate of 80% including 50% MRD-negative CR was achieved. At 12 months, 38% of evaluable patients remained progression-free and median OS was not reached. Patients who achieved an initial MRD-negative CR did not reach median PFS and were all alive at 1-year follow-up.

(See figure on next page.)

Fig. 3 Efficacy of HD-CAR-1 treatment and patient outcome. **A** Overall survival (OS) and **B** progression-free survival (PFS) of treated patients. **C** OS and **D** PFS at end of study (EOS) on day 90 after HD-CAR-1 CART administration of HD-CAR-1 patients that achieved complete remission (CR; blue) vs. non-responders (red; partial remission (PR), stable disease (SD), progressive disease (PD)). **E** Swimmer plot depicting the course of individual HD-CAR-1 patients. **F** OS and **G** PFS according to administered HD-CAR-1 CART dose (dose level (DL); DL1: 1×10^6 CARTs/ m^2 ($n=3$), DL2 5×10^6 CARTs/ m^2 ($n=3$), DL3 20×10^6 CARTs/ m^2 ($n=4$), DL4: 5×10^7 CARTs/ m^2 ($n=3$)). DL: dose level; CR: complete remission; and MRD (minimal residual disease). \blacktriangleright : CART therapy, \blacksquare : allogeneic stem cell transplantation, \blacklozenge : antibody treatment, \blacklozenge : chemotherapy, \blacksquare : progressive disease (PD), \blacksquare : partial remission (PR), \blacksquare : stable disease (SD), \blacksquare : MRD-positive complete remission (CR), \blacksquare : MRD-negative complete remission/metabolic CR (CR*), \dagger : death

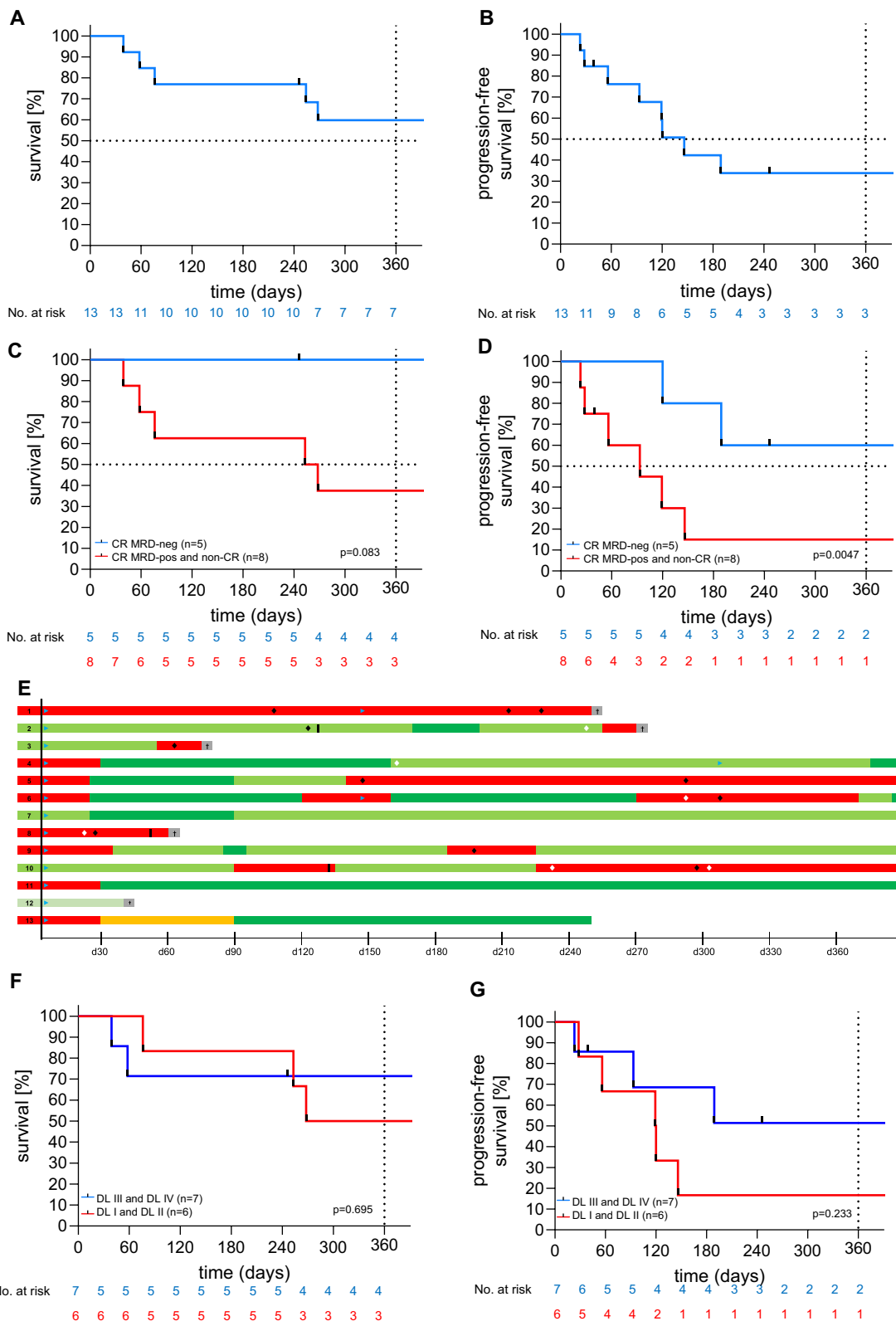


Fig. 3 (See legend on previous page.)

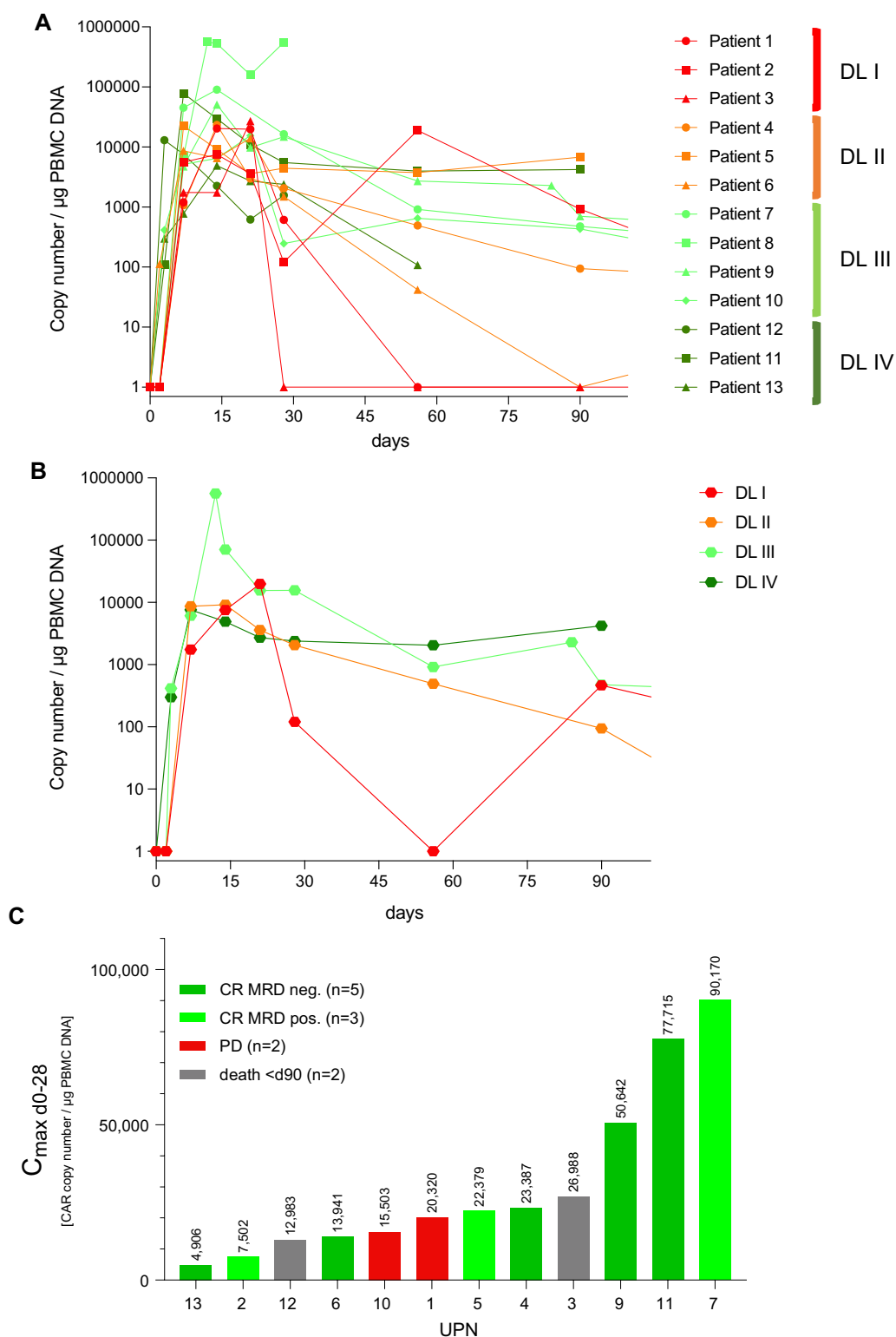


Fig. 4 Expansion of HD-CAR-1 CARTs. **A** Expansion of CARTs in the peripheral blood (PB) of individual HD-CAR-1 patients ($n=13$) assessed by single-copy gene duplex quantitative PCR (SCG-DP-PCR) [19] after CART administration and up to end of study (EOS) at day 90. **B** Median expansion of CARTs according to administered CART dose levels (DL; DL1: 1×10^6 CARTs/ m^2 , DL2: 5×10^6 CARTs/ m^2 , DL3: 20×10^6 CARTs/ m^2 , DL4: 5×10^7 CARTs/ m^2). **C** Maximum CART copies (c_{max}) within 28 days after CART administration and clinical response at EOS (data of UPN#8 not shown due to progressive disease on day 23 after CARTs). Median (c_{max}) 22.350 CART/ μg DNA PBMC. CR complete remission, d day, DL dose level, MRD minimal residual disease, PBMC peripheral blood mononuclear cell, PD progressive disease, UPN unique patient number

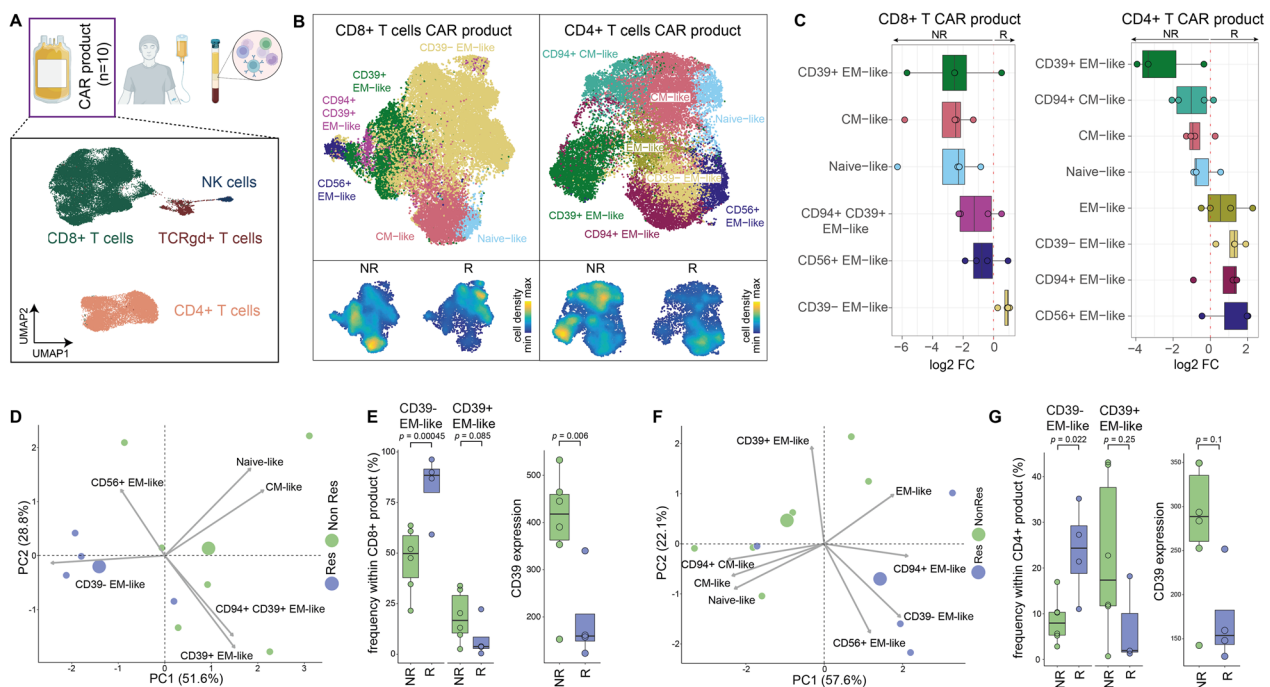


Fig. 5 Characterization of the cellular composition of CART products of HD-CAR-1 patients ($n = 10$). **A** CART infusion products were analyzed via high-parametric spectral flow cytometry, and data were analyzed (see methods). Uniform manifold approximation and projection (UMAP) visualization display a downsampled subset of cells from all ten CART products (bottom). After clustering, individual clusters were annotated based on surface marker expression [66] and highlighted by different colors. **B** CD8+ and CD4+ T cell subsets from the CART product of ten patient samples were extracted and clustered separately. A representative subset of cells from all ten CART products is displayed in the UMAP visualizations. Density plots in the two lower panels indicate the differential distribution of cells between non-responders (NR) and responders (R) within the CD8+ and CD4+ T cell compartment, respectively. **C** Boxplots indicating differential abundance of individual clusters from CD8+ (left) and CD4+ T cell (right) subsets from the CART product of responders and non-responders. Positive \log_2 fold changes indicate higher levels in responders, whereas negative \log_2 fold changes indicate that a specific population is more abundant in non-responders. **D** Principal component analysis (PCA) of CD8+ T cells within the CART product. Cell-type frequencies of cell clusters from each sample were used as input for the PCA. Blue circles represent samples from responders, and green circles represent samples from non-responders. The two larger circles indicate the midpoint of the respective group. Gray arrows indicate the variables. **E** Boxplots indicating the abundance of CD39- effector memory (EM)-like and CD39+ EM-like cells within the CD8+ T cell population of the CART products (left). A generalized linear mixed model (GLMM) was used to compute significance between non-responders and responders. Adjusted p values are shown. Boxplot of CD39 expression levels in non-responders and responders within the CD8+ T cell subset of the CART product is displayed (right). Significance was assessed by applying a linear mixed model (LMM). **F** PCA of CD4+ T cells within the CART product. Cell-type frequencies of cell clusters from each sample were used as input for the PCA. Blue circles represent samples from responders, and green circles represent samples from non-responders. The two larger circles indicate the midpoint of the respective group. Gray arrows indicate the variables. **G** Boxplots showing the abundance of CD39- EM-like and CD39+ EM-like cells within the CD4+ T cell population of the CART product (left). A GLMM was used to compute significance between non-responder and responder. Adjusted p values are shown. Boxplot of CD39 expression levels in non-responder and responder samples within the CD4+ T cell subset of the CAR product (right). Significance was assessed by applying a LMM. R responders, NR non-responders, CM central memory T cells, cDC conventional dendritic cells, EM effector memory T cells, NK natural killer

The CAR construct used within HD-CAR-1 has already been evaluated in the context of two clinical trials that focused on patients with non-Hodgkin's lymphoma (NHL). Also, five adult ALL patients ($n = 1$ [10], $n = 4$ [11]) were included. No response in the single ALL patient [10] and CR in 50% (two of four ALL patients) [11] were reported, although results were limited by the small patient number.

Result of HD-CAR-1 is in line with previous trials of second-generation CARTs in adult ALL patients: Park

et al. reported a CR rate of 83% ($n = 53$), with 50% OS and 30% event-free survival (EFS) one year after treatment [33]. In the ZUMA-3 trial resulting in the approval of Brexucabtagene autoleucel for treatment of adult r/r ALL patients in 2021, a CR rate of 71% ($n = 55$) with 12-month OS of 75% and EFS of 50% was observed. These results might be at least in part be attributable to the strict exclusion criteria in the ZUMA-3 trial of included patients [34]. Frey et al. reported a CR rate of 69% ($n = 35$) with OS of 47% and EFS of 31% at two-year follow-up. In

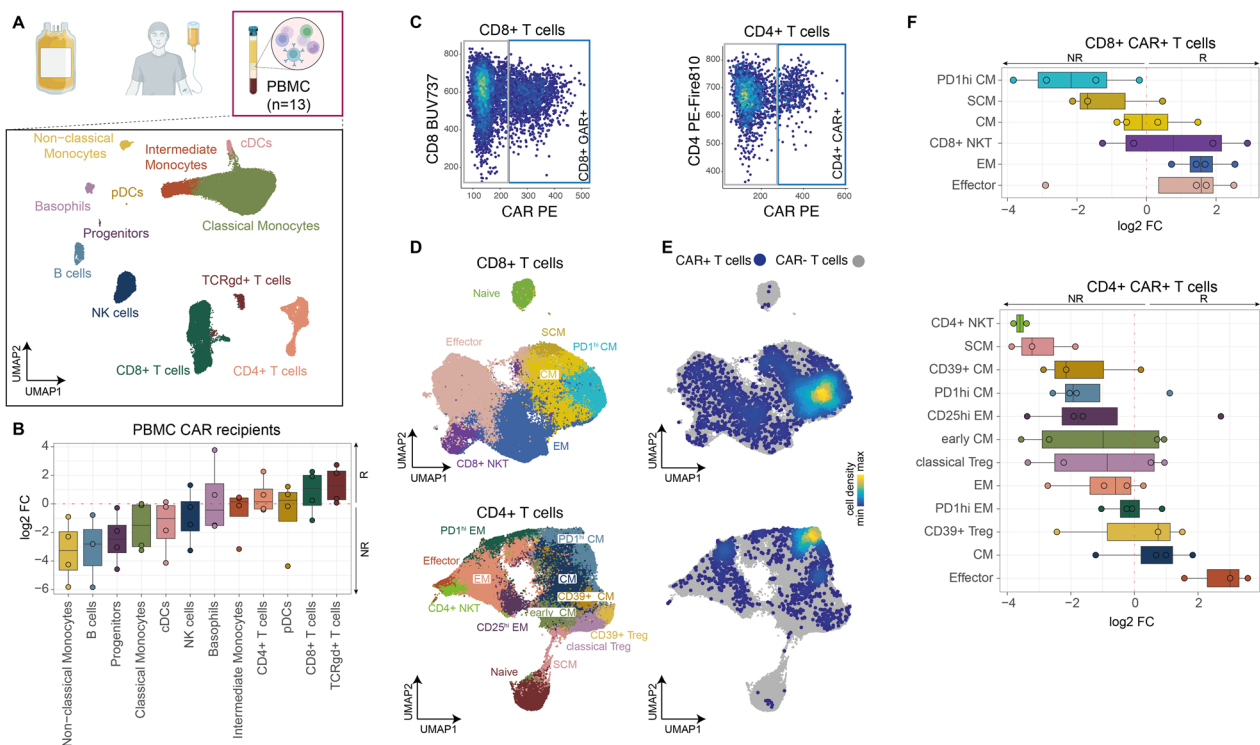


Fig. 6 Characterization of the cellular composition of PB samples ($n = 10$) of patients after HD-CAR-1 treatment ($n = 10$) and PB composition of healthy donors ($n = 3$). **A** PBMC samples obtained from patients after CART administration were analyzed via high-parametric spectral flow cytometry and data were analyzed (see methods). UMAP visualization (bottom) showing a downscaled subset of PBMCs from ten CART recipients and additionally three healthy donor samples. After clustering, individual clusters were annotated based on surface marker expression and highlighted by different colors. **B** Boxplots indicating differential abundance of individual cell populations from PBMC samples collected after CART administration, comparing abundances in responders and non-responders. Positive \log_2 fold changes indicate that a respective population is more abundant in responders (R), whereas negative \log_2 fold changes indicate that the population is more abundant in non-responders (NR). **C** Scatterplot displays the gating strategy to define CAR+ cells. CD8+ and CD4+ T cells from the PBMC samples were extracted, and fluorescence intensity levels of CD8/CD4 expression were plotted against the fluorescence intensity of the CAR targeting antibody. CAR+ cells were determined by setting a CD8+/CD4+ T cell-specific cutoff for downstream analysis and visualization. **D** UMAP visualizations of downscaled subsets from separately clustered CD8+ and CD4+ T cells identified in **A**. Dimensionality reduction and clustering were performed excluding the expression information of the CAR targeting antibody, to prevent CAR+ specific clusters. After clustering, individual clusters were annotated based on surface marker expression and highlighted by different colors. **E** Density plots illustrating the distribution of CAR+ cells within the CD8+ T cell (top) and CD4+ T cell (bottom) UMAP embedding. CAR+ cells were identified and gated as displayed in **C** and as described in the material and methods section. **F** CD4+ and CD8+ T cells from **D** were used and binned into CAR- and CAR+ CD8+ or CD4+ T cells, respectively, as described above (Fig. 5C). Boxplots display differential abundance of different CAR+ CD8+ T cells (top) or CAR+ CD4+ T cell phenotypes (bottom) of responders and non-responders. Positive \log_2 fold changes indicate that a respective population is more abundant in samples of responders, whereas negative \log_2 fold changes indicate that the population is more abundant in samples of non-responders. R responders, NR non-responders, CM central memory T cells, cDC conventional dendritic cells, EM effector memory T cells, hi high, TCR T cell receptor, NK natural killer, NKT natural killer T cells, pDC plasmacytoid dendritic cells, SCM memory stem cell-like T cells

this latter trial, high-dose (5×10^8), fractionated CART administration ($n = 20$) resulted in unmet median OS and EFS one year after treatment. Of note, only 25% of patients had received a prior alloSCT [35].

Relapses post-CARTs have been reported in 30 to 60% of ALL patients [33, 36–39]. Also in HD-CAR-1, 50% of patients with CR at EOS, have relapsed in the first year after treatment and three patients have received a consecutive alloSCT after HD-CAR-1 treatment. In line with data on the ZUMA-3 trial [34], efficacy of HD-CAR-1

CARTs was limited in patients with extramedullary disease: Only one patient (UPN #13) with extramedullary disease at CART treatment did not relapse after CART treatment, underlining the difficulties of treatment of this patient subgroup.

Of note, HD-CAR-1 appears to be associated with a highly favorable toxicity profile, even at high-dose levels: No ICANS or higher-grade CRS occurred, and only low-grade (I-II°) CRS was observed in 31% of the patients. Prior alloSCT was associated with fatal exacerbation of

a most likely preexisting GvHD in one patient. Although an immunogenic effect of CARTs cannot be excluded, GvHD might have been rather triggered substantially by preceding therapies including inotuzumab ozogamicin and blinatumomab.

As for hematotoxicity, the rate of prolonged neutropenia was comparable or lower than the one of previous reports [37, 40, 41], despite the high rate of patients after an alloSCT.

CD28-costimulation has been associated with rapid expansion and marked anti-tumor efficacy [42–44], and 4-1BB has been shown to enhance proliferation, to reduce exhaustion and to mediate long-term CART persistence [45–47]. In fact, we observed fast expansion of HD-CAR-1-CARTs. In contrast to loss of CARTs in the PB of patients treated in ZUMA-3 on day 28 [48], CARTs were durably detected in HD-CAR-1 patients. In line with others, initial MRD-negative response [38, 49] and higher doses of administered CARTs [35] resulted in higher CART frequencies and improved outcome.

High-resolution immunophenotyping revealed an immune cell repertoire of responders characterized by general activation of T cells. In contrast to others, we observed no influence on response by myeloid subtypes [11] or CD4+/CD8+ T cell ratio [50, 51]. Interestingly, the patient with the most durable response to treatment (UPN#11) displayed a distribution of immune cells in his PB which resembled the cellular composition of the PB of healthy donors. In patients responding to CART therapy, we observed a higher number of $\gamma\delta$ T cells within collected PBMCs. In fact, infiltration of malignancies with $\gamma\delta$ T cells is associated with favorable prognosis [52] and in the allo-SCT setting, $\gamma\delta$ T cells have been associated with enhanced anti-tumor response, improved OS and reduced occurrence of GvHD [53, 54].

Within the CART product, expression of CD39 on effector T cells predicted response: Low levels of this T cell subset were observed in responders, high levels in non-responders. CD39 is expressed on T cell subsets [55, 56], and its expression on CD8-positive T cells has been associated with T cell exhaustion [57, 58]. While CARTs with a less differentiated phenotype, e.g., central memory or naïve CARTs, mediate better expansion, persistence and antitumor activity [59, 60], T cell exhaustion is associated with inferior response [61, 62]. In the context of CARTs, CD39 expression has been linked to reduced CART expansion [63, 64]. Here, we confirm clinically that CD39 within the CART product might be highly relevant to predict outcome in CART patients. In contrast to other molecules such as PD-1 that have been identified not only in CART samples but also in healthy individuals [65], CD39 might constitute a more specific marker for T cell exhaustion.

Conclusion

In summary, administration of third-generation HD-CAR-1 CARTs was remarkably safe and of promising efficacy. Responses correlated with MRD clearance and were dose-dependent. Lack of CD39 expression on T cell subsets within the CART product was associated with improved anti-leukemic activity of CARTs. HD-CAR-1 appears to be a promising step toward safe and effective ALL eradication in older patients.

Abbreviations

AE	Adverse event
ALL	Acute lymphoblastic leukemia
alloSCT	Allogeneic stem cell transplantation
ASTCT	American Society for Transplantation and Cellular Therapy
BM	Bone marrow
CAR	Chimeric antigen receptor
CART	Chimeric antigen receptor T cells
CD	Cluster of differentiation
C_{max}	Maximal concentration
CMV	Cytomegalovirus
CR	Complete remission
CRS	Cytokine release syndrome
CTCAE	Common Terminology Criteria for Adverse Events
DIC	Disseminated intravascular coagulation
DL	Dose level
DLT	Dose-limiting toxicity
EBV	Epstein–Barr virus
EFS	Event-free survival
EOS	End of study
GI	Gastrointestinal
GLMM	Generalized linear mixed model
GMP	Good manufacturing practice
GvHD	Graft-versus-host disease
HD-CAR-1	Heidelberg CAR trial 1
HLH	Hemophagocytic lymphohistiocytosis
ICANS	Immune effector cell-associated neurotoxicity syndrome
IIT	Investigator-initiated trial
IL	Interleukin
LMM	Linear mixed model
MAS	Macrophage activation syndrome
MRD	Minimal residual disease
NHL	Non-Hodgkin lymphoma
n.r.	Not reached
NR	Non responder
OS	Overall survival
PB	Peripheral blood
PBMC	Peripheral blood mononuclear cell
PCA	Principal component analysis
PD	Progressive disease
PFS	Progression-free survival
PR	Partial remission
R	Responder
RSV	Respiratory syncytial virus
r/r	Refractory and/or relapsed
SD	Stable disease
SCG-DP-PCR	Single-copy gene-based duplex quantitative PCR
TLS	Tumor lysis syndrome
UKHD	Heidelberg University Hospital
UMAP	Uniform manifold approximation and projection
UPN	Unique patient number

Supplementary Information

The online version contains supplementary material available at <https://doi.org/10.1186/s13045-023-01470-0>.

Additional file 1. Table S.1 Antibodies used for assessment of cellular composition of CART products and of PB samples of patients after CART treatment. **Table S.2** Characterization of the leukapheresis and the HD-CAR-1 product by conventional flow cytometry. **Table S.3** HD-CAR-1 adverse events according to CTCAE. **Figure S.1** Structure of the RV-SFG. CD19.CD28.4-1BBzeta retroviral vector. **Figure S.2** Additional data on the cellular composition of CART products and of corresponding PB samples.

Acknowledgements

We thank the patients and their families.

Author contributions

MS is the principle investigator (PI) of the HD-CAR-1 clinical trial. PD is the deputy PI of the HD-CAR-1 clinical trial. MS, MLS, PD, AS, TS, CMT, GB, JS, FL, NG, JC, MG, JF, MRI, DW and MB treated patients. MS, MLS, AS, BN, AHK, LW, PWu, JK, PD, ADH, CMT, PW and AKul wrote and reviewed the HD-CAR-1 trial protocol. MS, AS, TS, BN, LW, MLS, JK, AHK, AKul, ADH and PD prepared the HD-CAR-1 trial, obtained approval from the local authorities to perform the trial and obtained the corresponding manufacturing license. MS, AS, BN, AH-K, AK, LW, BM and AKun are part of the GMP core facility of the Heidelberg University Hospital, manufactured HD-CAR-1 CART cells and performed quality control of the CART cell products. AS: PP and SLa were responsible for the leukapheresis unit. MLS, PW, AS, TS, PD and MS collected, organized, discussed and interpreted data. AKun, DH, MLS, AS and MS designed, performed and analyzed data on CAR T cell quantification. DV, SY, LJS and SH designed, performed, analyzed, wrote respective manuscript parts and generated figures on high-dimensional flow cytometry. MLS and MS wrote the primary manuscript. MLS, MS, PW, FK, PDe, DH, AS and LW designed and generated figures. MLS and PW designed and generated tables. All authors revised the work within this manuscript. All authors edited the manuscript and approved the final version for publication. All authors agreed to be accountable for all aspects included in this work.

Funding

Open Access funding enabled and organized by Projekt DEAL. This work was supported by the National Center of Tumor Diseases (NCT), by the German Cancer Research Institute (DKFZ), by the Jochen Siebeneicher Foundation and by a personal donation from Dr. h.c. Karl Schlecht. MLS is supported by the Olympia Morata Program of the Medical Faculty of the University of Heidelberg (grant no. OM 09/2019). AN is supported by the Carreras leukemia foundation (AH06-01). FL receives support from the Frankfurter Förderung "Nachwuchswissenschaftler" and the EUTOS funding program.

Availability of data and materials

The datasets used and/or analyzed within this study as well as materials are available from the corresponding author on request.

Declarations

Competing interests

AS: Travel grants from Hexal and Jazz Pharmaceuticals. Research grant from Therakos/Mallinckrodt. Consultancy BMS, Janssen-Cilag. Co-founder and part-time employee of TolerogenixX Ltd. of TolerogenixX Ltd. CMT: research support from Bayer AG. Advisory board member Pfizer, Janssen-Cilag GmbH. Grants and/or provision of investigational medicinal products from Pfizer, Daiichi Sankyo, BiolineRx. FL: Advisory roles for Novartis, Incyte, Sanofi Aventis and Bristol-Myers Squibb. GB: Research support from Novartis; Consultancy for Novartis, Pfizer, Gilead, Celgene; Honoraria from Jazz, Celgene, Gilead; Travel support from Neovii, Jazz, Gilead. JC: Travel grants: Pfizer, Ipsen, Medac; Adboard: Pfizer, Merck, Ipsen, MSD; Consultancy: Pfizer, Merck, Medac. JK: Consultancy Novartis, Global Blood Therapeutics, bluebird bio. MB: consulting fees from Amgen and PRMA, research funding from Amgen, honoraria/travel grants from Jazz, Celgene, Novartis, Pfizer and Amgen, advisory board member for Incyte and Amgen. MLS: consultancy for Kite/Gilead, Takeda.

MS: research grants from Apogenix, Hexal and Novartis. Travel grants from Hexal and Kite. Financial support for educational activities and conferences from bluebird bio, Kite and Novartis. Advisory board member of MSD. (Co-) PI of clinical trials of MSD, GSK, Kite and BMS. Co-Founder and shareholder of TolerogenixX Ltd. PD: consultancy AbbVie, AstraZeneca, Gilead, Janssen, Novartis, Riemser, Roche; speakers bureau AbbVie, Gilead, Novartis, Riemser, Roche; research support from Neovii and Riemser. None of the mentioned sources supported the work described within this manuscript. PDe: honorarium from MSD. PWu: Research support from the German Red Cross Blood Service Baden-Württemberg – Hessen gGmbH. Advisory Board Member of Sanofi-Aventis. TS: Consultant AbbVie, Takeda, Astellas, Amgen, Bristol-Myers Squibb, Gilead, Ridgeline Discoveries. Honorarium: Pfizer, AbbVie, Jazz Pharmaceuticals. Financial support congress participation: AbbVie, Jazz Pharmaceuticals., ADH, AHK, AKei, AKul, AKun, AN, BM, BN, DH, DV, DW, FK, JF, LJS, LW, MG, MRi, NG, PP, PW, SH, SLa, SY: none.

Author details

¹Department of Internal Medicine V, University Hospital Heidelberg, Im Neuenheimer Feld 410, 69120 Heidelberg, Germany. ²Heidelberg Institute for Stem Cell Technology and Experimental Medicine (HI-STEM gGmbH), Heidelberg, Germany. ³Division of Stem Cells and Cancer, Deutsches Krebsforschungszentrum (DKFZ) and DKFZ-ZMBH Alliance, Heidelberg, Germany. ⁴Faculty of Biosciences, Heidelberg University, Heidelberg, Germany. ⁵Berlin Institute of Health (BIH) at Charité – Universitätsmedizin Berlin, Berlin, Germany. ⁶Berlin Institute for Medical Systems Biology, Max Delbrück Center for Molecular Medicine in the Helmholtz Association, Berlin, Germany. ⁷Department of Hematology, Oncology and Tumor Immunology, Charité University Medicine, Berlin, Germany. ⁸Department of Pediatric Hematology, Oncology and Immunology, University Hospital Heidelberg, Heidelberg, Germany. ⁹Institute for Clinical Transfusion Medicine and Cell Therapy (IKTZ), German Red Cross Blood Service Baden-Württemberg-Hessen, Heidelberg, Germany. ¹⁰Institute of Transfusion Medicine and Immunology, Medical Faculty Mannheim, of the Heidelberg University, German Red Cross Blood Service Baden-Württemberg – Hessen, Mannheim, Germany. ¹¹GRN MVZ Sinsheim, Sinsheim, Germany. ¹²Department of Internal Medicine II, University Hospital Frankfurt, Frankfurt, Germany. ¹³Department of Hematology and Oncology, University Hospital Oldenburg, Oldenburg, Germany. ¹⁴Department of Hematology and Oncology, Hospital Bielefeld, Bielefeld, Germany. ¹⁵Department of Internal Medicine I, University Hospital Freiburg, Freiburg, Germany. ¹⁶Department of Hematology, Oncology and Immunology, University Hospital Giessen und Marburg, Marburg, Germany. ¹⁷Städtisches Klinikum Karlsruhe, Karlsruhe, Germany. ¹⁸Department of Hematology and Oncology, Center of Internal Medicine, Otto-von-Guericke University Medical Center, Magdeburg, Germany. ¹⁹Department of Internal Medicine II, University Hospital Kiel, Kiel, Germany. ²⁰German Cancer Consortium (DKTK) and German Cancer Research Center (DKFZ)/National Center for Tumor Diseases (NCT), Heidelberg, Germany.

Received: 28 February 2023 Accepted: 20 June 2023

Published online: 22 July 2023

References

1. European Medicines Agency. Yescarta - axicabtagene ciloleucel. 2022. Available from: <https://www.ema.europa.eu/en/medicines/human/EPAR/yescarta>.
2. European Medicines Agency. Kymriah - tisagenlecleucel. 2022. Available from: <https://www.ema.europa.eu/en/medicines/human/EPAR/kymriah>.
3. European Medicines Agency. Tecartus - brexucabtagene autoleucel. 2022. Available from: <https://www.ema.europa.eu/en/medicines/human/EPAR/tecartus>.
4. European Medicines Agency. Breyanzi - lisocabtagene maraleucel. 2022. Available from: <https://www.ema.europa.eu/en/medicines/human/EPAR/breyanzi>.
5. Carpenito C, Milone MC, Hassan R, Simonet JC, Lakhai M, Suhoski MM, et al. Control of large, established tumor xenografts with genetically retargeted human T cells containing CD28 and CD137 domains. *Proc Natl Acad Sci U S A*. 2009;106(9):3360–5.
6. Li W, Guo L, Rathi P, Marinova E, Gao X, Wu MF, et al. Redirecting T cells to glypican-3 with 4–1BB zeta chimeric antigen receptors results

- in Th1 polarization and potent antitumor activity. *Hum Gene Ther.* 2017;28(5):437–48.
7. Park S, Shevlin E, Vedyas Y, Zaman M, Park S, Hsu YS, et al. Micromolar affinity CART cells to ICAM-1 achieves rapid tumor elimination while avoiding systemic toxicity. *Sci Rep.* 2017;7(1):14366.
 8. Tammana S, Huang X, Wong M, Milone MC, Ma L, Levine BL, et al. 4–1BB and CD28 signaling plays a synergistic role in redirecting umbilical cord blood T cells against B-cell malignancies. *Hum Gene Ther.* 2010;21(1):75–86.
 9. Zhong XS, Matsushita M, Plotkin J, Riviere I, Sadelain M. Chimeric antigen receptors combining 4–1BB and CD28 signaling domains augment PI3kinase/AKT/Bcl-XL activation and CD8+ T cell-mediated tumor eradication. *Mol Ther.* 2010;18(2):413–20.
 10. Ramos CA, Rouce R, Robertson CS, Reyna A, Narala N, Vyas G, et al. In vivo fate and activity of second- versus third-generation CD19-specific CAR-T cells in B Cell Non-Hodgkin's Lymphomas. *Mol Ther.* 2018;26(12):2727–37.
 11. Enblad G, Karlsson H, Gammelmård G, Wenthe J, Lövgren T, Amini RM, et al. A phase I/IIa trial using CD19-targeted third-generation CAR T cells for lymphoma and leukemia. *Clin Cancer Res.* 2018;24(24):6185–94.
 12. Schubert ML, Schmitt A, Sellner L, Neuber B, Kunz J, Wuchter P, et al. Treatment of patients with relapsed or refractory CD19+ lymphoid disease with T lymphocytes transduced by RV-SFG.CD19.CD28.4–1BBzeta retroviral vector: a unicentre phase I/II clinical trial protocol. *BMJ Open.* 2019;9(5):e026644.
 13. Wang L, Gong W, Wang S, Neuber B, Sellner L, Schubert ML, Hückelhoven-Krauss A, Kunz A, Gern U, Michels B, Hinkelbein M, Mechler S, Richter P, Müller-Tidow C, Schmitt M, Schmitt A. Improvement of in vitro potency assays by a resting step for clinical-grade chimeric antigen receptor engineered T cells. *Cytotherapy.* 2019;21(5):566–78. <https://doi.org/10.1016/j.jcyt.2019.02.013>.
 14. Lee DW, Santomaso BD, Locke FL, Ghobadi A, Turtle CJ, Brudno JN, et al. ASTCT consensus grading for cytokine release syndrome and neurologic toxicity associated with immune effector cells. *Biol Blood Marrow Transplant.* 2019;25(4):625–38.
 15. Schubert ML, Schmitt M, Wang L, Ramos CA, Jordan K, Müller-Tidow C, et al. Side-effect management of chimeric antigen receptor (CAR) T-cell therapy. *Ann Oncol.* 2021;32(1):34–48.
 16. Cairo MS, Bishop M. Tumour lysis syndrome: new therapeutic strategies and classification. *Br J Haematol.* 2004;127(1):3–11.
 17. Appelbaum FR, Rosenblum D, Arcenci RJ, Carroll WL, Breitfeld PP, Forman SJ, et al. End points to establish the efficacy of new agents in the treatment of acute leukemia. *Blood.* 2007;109(5):1810–6.
 18. Cheson BD, Pfistner B, Juweid ME, Gascoyne RD, Specht L, Horning SJ, et al. Revised response criteria for malignant lymphoma. *J Clin Oncol.* 2007;25(5):579–86.
 19. Kunz A, Gern U, Schmitt A, Neuber B, Wang L, Hückelhoven-Krauss A, et al. Optimized assessment of qPCR-based vector copy numbers as a safety parameter for GMP-grade CAR T cells and monitoring of frequency in patients. *Mol Ther Methods Clin Dev.* 2020;17:448–54.
 20. Ashhurst TM, Marsh-Wakefield F, Putri GH, Spiteri AG, Shinko D, Read MN, et al. Integration, exploration, and analysis of high-dimensional single-cell cytometry data using Spectre. *Cytometry A.* 2021;101:237–53.
 21. Nowicka M, Krieg C, Crowell HL, Weber LM, Hartmann FJ, Guglietta S, et al. CyTOF workflow: differential discovery in high-throughput high-dimensional cytometry datasets. *F1000Res.* 2017;6:748.
 22. Weber LM, Nowicka M, Soneson C, Robinson MD. diffcyt: Differential discovery in high-dimensional cytometry via high-resolution clustering. *Commun Biol.* 2019;2:183.
 23. Van Gassen S, Gaudilliere B, Angst MS, Saeys Y, Aghaeepour N. CytoNorm: a normalization algorithm for cytometry data. *Cytometry A.* 2020;97(3):268–78.
 24. McInnes L, Healy J, Saul N, Großberger L. UMAP: uniform manifold approximation and projection. *J Open Source Softw.* 2018;3:861.
 25. Benjamini Y, Hochberg Y. Controlling the false discovery rate: a practical and powerful approach to multiple testing. *J R Stat Soc Ser B.* 1995;57:289–300.
 26. Lerner KG, Kao GF, Storb R, Buckner CD, Clift RA, Thomas ED. Histopathology of graft-vs.-host reaction (GVHR) in human recipients of marrow from HL-A-matched sibling donors. *Transpl Proc.* 1974;6(4):367–71.
 27. Aldoss I, Otoukesh S, Zhang J, Mokhtari S, Ngo D, Mojtahedzadeh M, et al. Extramedullary disease relapse and progression after blinatumomab therapy for treatment of acute lymphoblastic leukemia. *Cancer.* 2021;128:529–35.
 28. Gökbuğten N, Dombret H, Bonifacio M, Reichle A, Graux C, Faul C, et al. Blinatumomab for minimal residual disease in adults with B-cell precursor acute lymphoblastic leukemia. *Blood.* 2018;131(14):1522–31.
 29. Topp MS, Gökbuğten N, Stein AS, Zugmaier G, O'Brien S, Bargou RC, et al. Safety and activity of blinatumomab for adult patients with relapsed or refractory B-precursor acute lymphoblastic leukaemia: a multicentre, single-arm, phase 2 study. *Lancet Oncol.* 2015;16(1):57–66.
 30. Gokbuğten N. Treatment of older patients with acute lymphoblastic leukemia. *Hematology Am Soc Hematol Educ Program.* 2016;2016(1):573–9.
 31. Gokbuğten N, Dombret H, Ribera JM, Fielding AK, Advani A, Bassan R, et al. International reference analysis of outcomes in adults with B-precursor Ph-negative relapsed/refractory acute lymphoblastic leukemia. *Haematologica.* 2016;101(12):1524–33.
 32. Paul S, Kantarjian H, Jabbour EJ. Adult acute lymphoblastic leukemia. *Mayo Clin Proc.* 2016;91(11):1645–66.
 33. Park JH, Riviere I, Gonen M, Wang X, Sénéchal B, Curran KJ, et al. Long-term follow-up of CD19 CAR therapy in acute lymphoblastic leukemia. *N Engl J Med.* 2018;378:449–59.
 34. Shah BD, Ghobadi A, Oluwole OO, Logan AC, Boissel N, Cassaday RD, et al. KTE-X19 for relapsed or refractory adult B-cell acute lymphoblastic leukaemia: phase 2 results of the single-arm, open-label, multicentre ZUMA-3 study. *Lancet.* 2021;398(10299):491–502.
 35. Frey NV, Shaw PA, Hexner EO, Pequignot E, Gill S, Luger SM, et al. Optimizing chimeric antigen receptor T-cell therapy for adults with acute lymphoblastic leukemia. *J Clin Oncol.* 2020;38(5):415–22.
 36. Gardner RA, Finney O, Annesley C, Brakke H, Summers C, Leger K, et al. Intent-to-treat leukemia remission by CD19 CAR T cells of defined formulation and dose in children and young adults. *Blood.* 2017;129(25):3322–31.
 37. Maude SL, Laetsch TW, Buechner J, Rives S, Boyer M, Bittencourt H, et al. Tisagenlecleucel in children and young adults with B-cell lymphoblastic leukemia. *N Engl J Med.* 2018;378(5):439–48.
 38. Pulsipher MA, Han X, Maude SL, Laetsch TW, Qayed M, Rives S, et al. Next-generation sequencing of minimal residual disease for predicting relapse after tisagenlecleucel in children and young adults with acute lymphoblastic leukemia. *Blood Cancer Discov.* 2022;3(1):66–81.
 39. Hay KA, Gauthier J, Hirayama AV, Voutsinas JM, Wu Q, Li D, et al. Factors associated with durable EFS in adult B-cell ALL patients achieving MRD-negative CR after CD19 CAR T-cell therapy. *Blood.* 2019;133(15):1652–63.
 40. Fried S, Avigdor A, Bielorai B, Meir A, Besser MJ, Schachter J, et al. Early and late hematologic toxicity following CD19 CAR-T cells. *Bone Marrow Transplant.* 2019;54(10):1643–50.
 41. Schubert ML, Dietrich S, Stilgenbauer S, Schmitt A, Pavel P, Kunz A, et al. Feasibility and safety of CD19 chimeric antigen receptor T cell treatment for B cell lymphoma relapse after allogeneic hematopoietic stem cell transplantation. *Biol Blood Marrow Transplant.* 2020;26(9):1575–80.
 42. Kowolik CM, Topp MS, Gonzalez S, Pfeiffer T, Olivares S, Gonzalez N, et al. CD28 costimulation provided through a CD19-specific chimeric antigen receptor enhances in vivo persistence and antitumor efficacy of adoptively transferred T cells. *Cancer Res.* 2006;66(22):10995–1004.
 43. Loskog A, Giandomenico V, Rossig C, Pule M, Dotti G, Brenner MK. Addition of the CD28 signaling domain to chimeric T-cell receptors enhances chimeric T-cell resistance to T regulatory cells. *Leukemia.* 2006;20(10):1819–28.
 44. Zhao Z, Condomines M, van der Stegen SJC, Perna F, Kloss CC, Gunset G, et al. Structural design of engineered costimulation determines tumor rejection kinetics and persistence of CAR T cells. *Cancer Cell.* 2015;28(4):415–28.
 45. Long AH, Haso WM, Shern JF, Wanhainen KM, Murgai M, Ingaramo M, et al. 4–1BB costimulation ameliorates T cell exhaustion induced by tonic signaling of chimeric antigen receptors. *Nat Med.* 2015;21(6):581–90.
 46. Milone MC, Fish JD, Carpenito C, Carroll RG, Binder GK, Teachey D, et al. Chimeric receptors containing CD137 signal transduction domains mediate enhanced survival of T cells and increased antileukemic efficacy in vivo. *Mol Ther.* 2009;17(8):1453–64.
 47. Zhang H, Snyder KM, Suhoski MM, Maus MV, Kapoor V, June CH, et al. 4–1BB is superior to CD28 costimulation for generating CD8+

- cytotoxic lymphocytes for adoptive immunotherapy. *J Immunol.* 2007;179(7):4910–8.
48. Shah BD, Bishop MR, Oluwole OO, Logan AC, Baer MR, Donnellan WB, et al. KTE-X19 anti-CD19 CAR T-cell therapy in adult relapsed/refractory acute lymphoblastic leukemia: ZUMA-3 phase 1 results. *Blood.* 2021;138(1):11–22.
 49. Dourthe ME, Rabian F, Yakouben K, Chevillon F, Cabannes-Hamy A, Méchinaud F, et al. Determinants of CD19-positive vs CD19-negative relapse after tisagenlecleucel for B-cell acute lymphoblastic leukemia. *Leukemia.* 2021;35(12):3383–93.
 50. Turtle CJ, Hanafi LA, Berger C, Gooley TA, Cherian S, Hudecek M, et al. CD19 CAR-T cells of defined CD4+:CD8+ composition in adult B cell ALL patients. *J Clin Invest.* 2016;126(6):2123–38.
 51. Sommermeyer D, Hudecek M, Kosasih PL, Gogishvili T, Maloney DG, Turtle CJ, et al. Chimeric antigen receptor-modified T cells derived from defined CD8+ and CD4+ subsets confer superior antitumor reactivity in vivo. *Leukemia.* 2016;30(2):492–500.
 52. Gentles AJ, Newman AM, Liu CL, Bratman SV, Feng W, Kim D, et al. The prognostic landscape of genes and infiltrating immune cells across human cancers. *Nat Med.* 2015;21(8):938–45.
 53. Lamb LS Jr, Henslee-Downey PJ, Parrish RS, Godder K, Thompson J, Lee C, et al. Increased frequency of TCR gamma delta + T cells in disease-free survivors following T cell-depleted, partially mismatched, related donor bone marrow transplantation for leukemia. *J Hematother.* 1996;5(5):503–9.
 54. Godder KT, Henslee-Downey PJ, Mehta J, Park BS, Chiang KY, Abhyankar S, et al. Long term disease-free survival in acute leukemia patients recovering with increased gammadelta T cells after partially mismatched related donor bone marrow transplantation. *Bone Marrow Transplant.* 2007;39(12):751–7.
 55. Borsellino G, Kleinewietfeld M, Di Mitri D, Sternjak A, Diamantini A, Giometto R, et al. Expression of ectonucleotidase CD39 by Foxp3+ Treg cells: hydrolysis of extracellular ATP and immune suppression. *Blood.* 2007;110(4):1225–32.
 56. Deaglio S, Dwyer KM, Gao W, Friedman D, Usheva A, Erat A, et al. Adenosine generation catalyzed by CD39 and CD73 expressed on regulatory T cells mediates immune suppression. *J Exp Med.* 2007;204(6):1257–65.
 57. Gupta PK, Godec J, Wolski D, Adland E, Yates K, Pauken KE, et al. CD39 Expression identifies terminally exhausted CD8+ T cells. *PLoS Pathog.* 2015;11(10):e1005177.
 58. Qi Y, Xia Y, Lin Z, Qu Y, Qi Y, Chen Y, et al. Tumor-infiltrating CD39(+) CD8(+) T cells determine poor prognosis and immune evasion in clear cell renal cell carcinoma patients. *Cancer Immunol Immunother.* 2020;69(8):1565–76.
 59. Fraietta JA, Lacey SF, Orlando EJ, Pruteanu-Malinici I, Gohil M, Lundh S, et al. Determinants of response and resistance to CD19 chimeric antigen receptor (CAR) T cell therapy of chronic lymphocytic leukemia. *Nat Med.* 2018;24(5):563–71.
 60. Frigault MJ, Lee J, Basil MC, Carpenito C, Motohashi S, Scholler J, et al. Identification of chimeric antigen receptors that mediate constitutive or inducible proliferation of T cells. *Cancer Immunol Res.* 2015;3(4):356–67.
 61. Bai Z, Woodhouse S, Zhao Z, Arya R, Govek K, Kim D, et al. Single-cell antigen-specific landscape of CAR T infusion product identifies determinants of CD19-positive relapse in patients with ALL. *Sci Adv.* 2022;8(23):eabj2820.
 62. Deng Q, Han G, Puebla-Osorio N, Ma MCJ, Strati P, Chasen B, et al. Characteristics of anti-CD19 CAR T cell infusion products associated with efficacy and toxicity in patients with large B cell lymphomas. *Nat Med.* 2020;26(12):1878–87.
 63. Myers RM, Tarasiewicz A, Steinberg SM, Lambie AJ, Sheppard J, Yates B, et al. Blinatumomab nonresponse and high-disease burden are associated with inferior outcomes after CD19-CAR for B-ALL. *J Clin Oncol Off J Am Soc Clin Oncol.* 2022;40(9):932–44.
 64. Roselli E, Boucher JC, Li G, Kotani H, Spittler K, Reid K, et al. 4–1BB and optimized CD28 co-stimulation enhances function of human mono-specific and bi-specific third-generation CAR T cells. *J Immunother Cancer.* 2021;9(10).
 65. Duraiswamy J, Ibegbu CC, Masopust D, Miller JD, Araki K, Doho GH, et al. Phenotype, function, and gene expression profiles of programmed death-1(hi) CD8 T cells in healthy human adults. *J Immunol.* 2011;186(7):4200–12.
 66. Triana S, Vonficht D, Jopp-Saile L, Raffel S, Lutz R, Leonce D, et al. Single-cell proteo-genomic reference maps of the hematopoietic system enable the purification and massive profiling of precisely defined cell states. *Nat Immunol.* 2021;22(12):1577–89.

Publisher's Note

Springer Nature remains neutral with regard to jurisdictional claims in published maps and institutional affiliations.

Ready to submit your research? Choose BMC and benefit from:

- fast, convenient online submission
- thorough peer review by experienced researchers in your field
- rapid publication on acceptance
- support for research data, including large and complex data types
- gold Open Access which fosters wider collaboration and increased citations
- maximum visibility for your research: over 100M website views per year

At BMC, research is always in progress.

Learn more biomedcentral.com/submissions

